We are IntechOpen, the world's leading publisher of Open Access books
Built by scientists, for scientists

4,400
Open access books available

117,000
International authors and editors

130M
Downloads

Our authors are among the

154
Countries delivered to

TOP 1%
most cited scientists

12.2%
Contributors from top 500 universities

CLARIVATE ANALYTICS
BOOK CITATION INDEX
INDEXED

WEB OF SCIENCE™

Selection of our books indexed in the Book Citation Index in Web of Science™ Core Collection (BKCI)

Interested in publishing with us?
Contact book.department@intechopen.com

Numbers displayed above are based on latest data collected.
For more information visit www.intechopen.com

13

Silicon Carbide Neutron Detectors

Fausto Franceschini* and Frank H. Ruddy**
*Westinghouse Electric Company LLC, Research and Technology Unit,
Cranberry Township, Pennsylvania 16066 USA
**Ruddy Consulting, 2162 Country Manor Dr., Mt. Pleasant,
South Carolina 29466 USA

1. Introduction

The potential of Silicon Carbide (SiC) for use in semiconductor nuclear radiation detectors has been long recognized. In fact, the first SiC neutron detector was demonstrated more than fifty years ago (Babcock, *et al*., 1957; Babcock & Chang, 1963). This detector was shown to be operational in limited testing at temperatures up to 700 ^{o}C. Unfortunately, further development was limited by the poor material properties of SiC available at the time.

During the 1990's, much effort was concentrated on improving the properties of SiC by reducing defects produced during the crystal growing process such as dislocations, micropipes, *etc*. These efforts resulted in the availability of much higher quality SiC semiconductor materials. A parallel effort resulted in improved SiC electronics fabrication techniques.

In response to these development efforts, interest in SiC nuclear radiation detectors was rekindled in the mid 1990's. Keys to this interest are the capability of SiC detectors to operate at elevated temperatures and withstand radiation-induced damage better than conventional semiconductor detectors such as those based on Silicon or Germanium. These properties of SiC are particularly important in nuclear reactor applications, where high-temperature, high-radiation measurement environments are typical.

SiC detectors have now been demonstrated for high-resolution alpha particle and X-ray energy spectrometry, beta ray detection, gamma-ray detection, thermal- and fast-neutron detection, and fast-neutron energy spectrometry.

In the present chapter, emphasis will be placed on SiC neutron detectors and applications of these detectors. The history of SiC detector development will be reviewed, design characteristics of SiC neutron detectors will be outlined, SiC neutron detector applications achieved to date will be referenced and the present status and future prospects for SiC neutron detectors will be discussed.

2. Background

The initial efforts to develop SiC radiation detectors were directed towards neutron monitoring in nuclear reactors (Babcock, *et al.*, 1957; Babcock & Chang, 1963). Reactor neutron monitoring must often be carried out in high-temperature environments and intense radiation fields which lead to detector radiation damage concerns. Using crude detectors constructed by applying resistive contacts to SiC crystals, the authors were able to demonstrate detection of alpha particles. In anticipation of the high-temperature monitoring locations that would be encountered in nuclear reactors, these measurements were extended to temperatures up to 700 ^{o}C with only minimal changes in the detector response.

In follow-on work (Ferber & Hamilton, 1965), a SiC p-n diode coated with ^{235}U was exposed to thermal neutrons in a low-power research reactor. Good agreement was observed between the axial neutron flux profile measurements made with conventional gold-foil activation methods and the SiC detector measurements. The SiC neutron detector was also shown to have a linear response to reactor power in the 0.1 W to 1 kW range. Detector alpha response was observed to be acceptable after a thermal-neutron fluence of 6 x 10^{13} cm^{-2}.

Further development of SiC detectors was hindered by the poor quality of the available SiC materials available at the time.

Efforts at developing SiC detectors were renewed by Tikhomirova and co-workers in 1972 (Tikhomirova, *et al.*, 1972; Tikhomirova, *et al.*, 1973a; Tikhomirova, *et al.*, 1973b). Beryllium diffused 6H-SiC detectors with low, 1 nanoampere leakage currents were shown to be capable of 8% energy resolution for 4.8 MeV alpha particles (Tikhomirova, *et al.*, 1972).

The effects of neutron damage on a ^{235}U-coated, beryllium-diffused 6H-SiC diode were examined (Tikhomirova, *et al.*, 1973b). The detector response did not change significantly up to a thermal-neutron fluence of 10^{13} n cm^{-2}. At higher neutron fluences, the detector count rate decreased dramatically. The observed response changes were likely a result of fission-fragment induced radiation damage in the detector. The fission-fragment dose corresponding to a thermal-neutron fluence of 10^{13} cm^{-2} is approximately 10^{8} cm^{-2}.

Increases in SiC detector leakage currents as a result of neutron irradiation were reported by Evstropov, *et al.*, 1993.

In the 1990's, long-term development work resulted in the demonstration of technologies for producing high-quality SiC both in chemical vapour deposited (CVD) and large-wafer form. As a result of this development, some of the last major obstacles to commercial fabrication of high-performance SiC semiconductor devices were overcome.

The first use of these developments in high-quality CVD epitaxial SiC detectors was by Ruddy, *et al.*, 1998. Si substrate layers doped with n^{-} donor atoms (nitrogen) were overlayered with a lightly doped epitaxial layer containing a nitrogen concentration of 10^{15} cm^{-3}. The epitaxial layer thicknesses ranged from 3 μm to 8 μm. Detectors with 200 μm and 400 μm diameters were tested. Although detectors with diameters up to 1 mm were fabricated, the presence of defects in the form of micropipes limited the performance of

detectors with diameters greater than 400 μm. Nickel Schottky metal contacts covered by gold were applied to the epitaxial layers to form Schottky diodes, and thin (1 μm) p+ layers were applied to the n^- epitaxial layers to form p-n junction detectors. Both the Schottky diodes and p-n junctions were demonstrated as alpha detectors with ^{238}Pu sources. No drift in the pulse-height response was observed in the temperature range from 18 ^oC to 89 ^oC.

Similar results were reported by Nava, *et al.*, 1999. Alpha-particle response measurements were carried out for ^{241}Am using Schottky diodes fabricated on 4H-SiC epitaxial layers. Charge-carrier collection efficiency was shown to increase linearly with the square root of the detector reverse bias.

Rapid development of epitaxial SiC ensued leading to the development of high-resolution SiC alpha detectors (Ivanov, *et al.*, 2004; Ruddy, *et al.*, 2009b), high-resolution and temperature insensitive X-ray detectors (Bertuccio, *et al*, 2001; Bertuccio, *et al*, 2003; Bertuccio, *et al*, 2004a; Bertuccio, *et al*, 2004b; Bertuccio, *et al*, 2005; Bertuccio, *et al*, 2010, Phlips, *et al.*, 2006; Lees, *et al.*, 2007) and detectors for minimum ionizing particles (Bruzzi, *et al.*, 2003: Moscatelli, *et al.,* 2006) as well as neutron detectors, which will be emphasized in this chapter.

High-quality SiC diodes are now readily available with diameters up to 6 mm and depletion layer thicknesses of 100 μm (Ruddy, *et al.*, 2009a)

Epitaxial SiC detectors have also been shown to operate reliably in ambient temperatures up to 375 ^oC (Ivanov, *et al.*, 2009).

Comprehensive reviews of SiC detector design and development can be found in Nava, *et al.*, 1998 and Strokan, *et al.*, 2009.

3. Silicon Carbide Nuclear Radiation Detectors

3.1 Silicon Carbide Neutron Detector Design

SiC neutron detectors are usually based on Schottky or p-n diodes. (Ruddy, *et al*, 1998; Nava, *et al.*, 1999; Manfredotti, *et al.*, 2005) A schematic drawing of a SiC Schottky diode detector is shown in Figure 1. The SiC substrate layer consists of high-purity material containing a residual n^+ doping concentration that is typically about 10^{18} cm^{-3} of nitrogen. The epitaxial layer is applied to the substrate layer and contains a much lower nitrogen concentration, typically 10^{14} – 10^{15} cm^{-3}. Lower n^- concentrations are necessary if the thickness of the epitaxial layer is greater than 10 μm in order to limit the voltage required to fully deplete the layer and collect the radiation-induced charge from this layer. An ohmic back contact and a Schottky front contact are applied. The front contact typically consists of a thin layer of titanium or nickel (~800 Å) covered by thicker layers of platinum (~1000 Å) and gold (~9000 Å). (see, for example, Ruddy, *et al.* [2006]) The thicker layers are needed to protect and ruggedize the Schottky metal layer. The optional convertor layer is used to obtain increased neutron sensitivity.

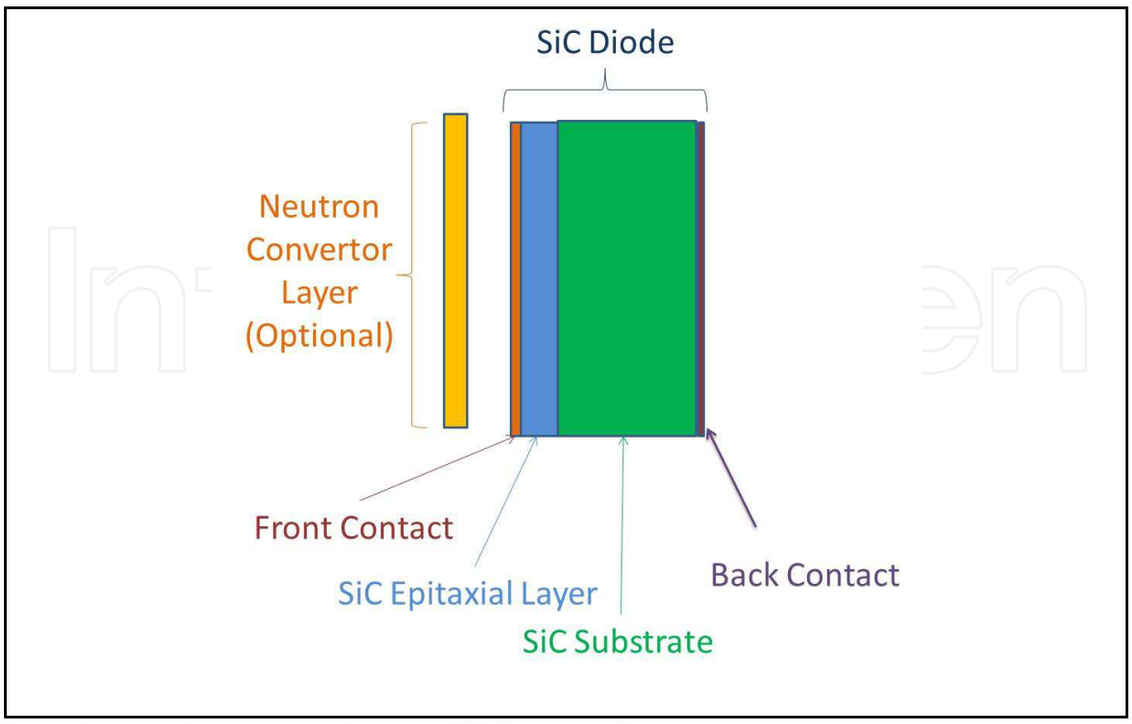

Fig. 1. Schematic representation of a SiC Schottky diode.

3.2 Silicon Carbide Thermal and Epithermal Neutron Detectors

A convertor layer with high thermal-neutron and epithermal-neutron cross sections is juxtaposed in front of the detector. In this way the likelihood of neutron-induced nuclear reactions leading to detectable ionization within the detector active volume is enhanced. For example, ^{6}Li has a thermal neutron cross section of 941 barns and can be used as a thin juxtaposed ^{6}Li layer as depicted in Figure 2.

Thermal neutrons interact with ^{6}Li to produce the following reaction:

$$^{6}\text{Li} + \text{n} \rightarrow {}^{4}\text{He} + {}^{3}\text{H}$$

The energetic alphas (^{4}He) and tritons (^{3}H) produced in the reaction can enter the detector active volume (epitaxial layer) and produce ionization in the form of electron-hole pairs. When a reverse bias voltage is applied to the detector as shown in Figure 2, the ionization is collected in the form of a charge pulse, which comprises the detector response signal. The tritons and alpha particles both contribute to the detector response as shown by the pulse-height spectrum in Figure 3 (Ruddy, *et al.,* 1996).

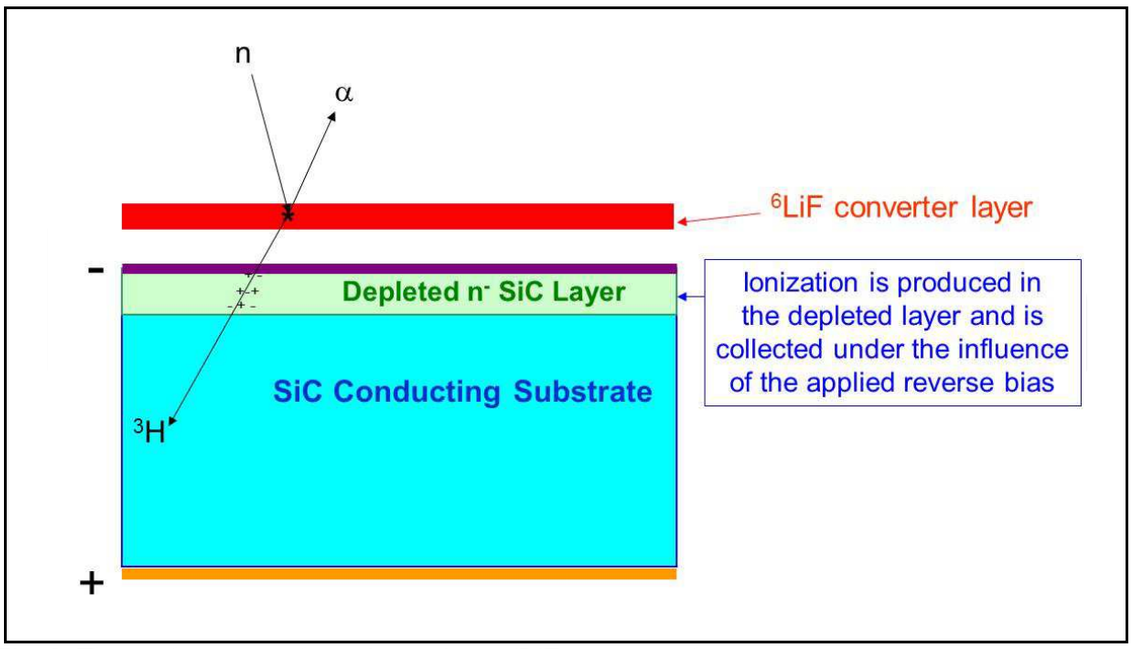

Fig. 2. Thermal neutron detection using a ^{6}LiF convertor layer.

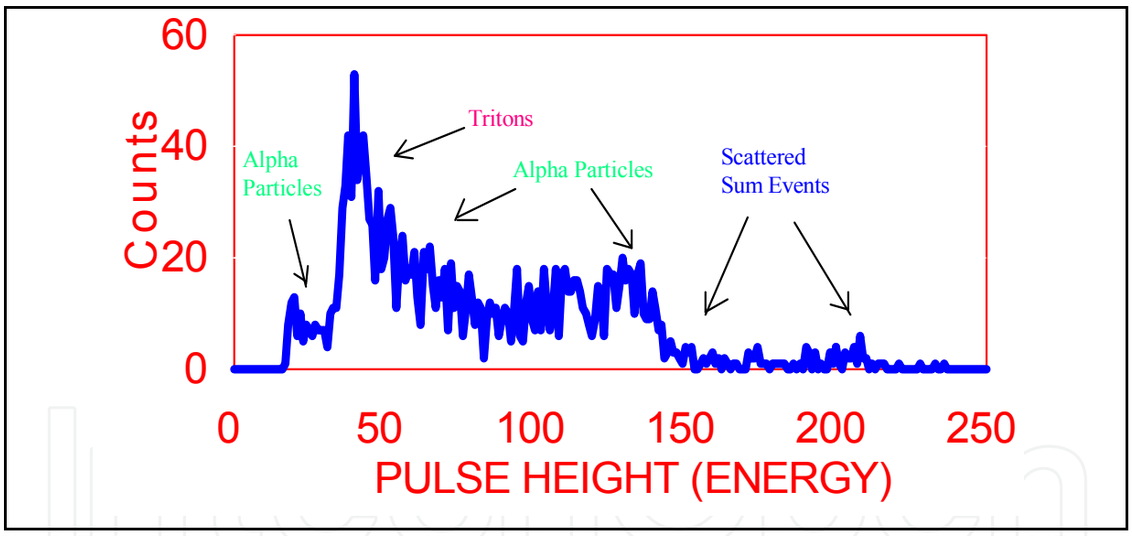

Fig. 3. Pulse height response for a 3-μm thick Schottky diode placed next to a thin ^{6}LiF layer and exposed to thermal neutrons (data from Ruddy, *et al.*, 1996).

Other nuclides with high neutron cross sections, such as ^{10}B and ^{235}U, can also be used in converter layers. The pulse-height response for a $Zr^{10}B_2$ layer positioned adjacent to a Schottky diode with a 3-μm active layer is shown in Figure 4 (Ruddy, *et al.*, 1996). The response is to charged particles from the following reaction:

$$^{10}B + n \rightarrow {}^7Li + {}^4He$$

Both ^{7}Li and ^{4}He ions are present in the spectrum. Two reaction branches are observed corresponding to production of ^{7}Li in the ground state (E_α = 1.78 MeV) and production of a 0.48-MeV excited state in ^{7}Li (E_α = 1.47 MeV). The former branch occurs in 6% of the reactions, whereas 94% populate the excited state.

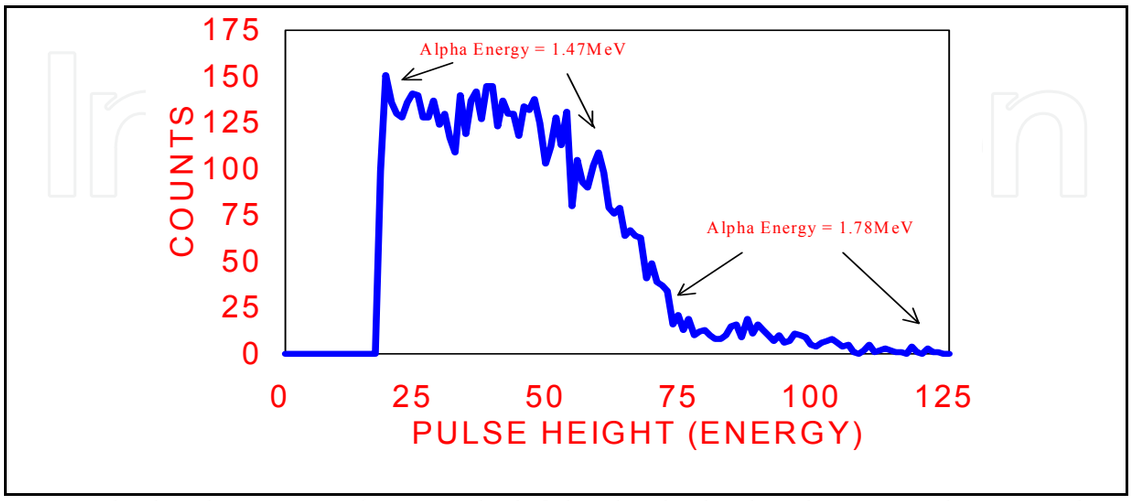

Fig. 4. Pulse height response for a 3-μ thick Schottky diode placed next to a thin $Zr^{10}B_2$ layer and exposed to thermal neutrons (data from Ruddy, *et al.*, 1996).

The pulse-height response for a thin ^{235}U layer placed adjacent to a Schottky diode with a 3-μm active layer is shown in Figure 5 (Ruddy, *et al.*, 1996). In this case, the pulse-height response is primarily to energetic fission fragments from thermal-neutron induced fission of ^{235}U. The fission process is asymmetric resulting predominantly in two fission fragments with different mass and kinetic energy: a heavy-mass peak with an average mass of 139 amu and average energy of 56.6 MeV and a low-mass peak with an average mass of 95 amu and an average energy of 93.0 MeV. Both peaks are clearly visible in the pulse-height spectrum. An additional low pulse-height peak is also visible. This peak is produced by alpha decay of the U^{235} enriched uranium used as the converter. Alpha particles from the decay of both ^{234}U and ^{235}U contribute to this peak.

^{235}U provides by far the most robust pulse-height response. However, the highly charged and energetic fission fragments produce a large amount of radiation damage in the detector active volume: the charge trapping sites produced by dislocation of the Si and C atoms from their original lattice positions degrade the pulse-height spectrum thereby limiting the service lifetime of the detector.

Although one may anticipate that ^{10}B with a thermal-neutron cross section of 3838 barns would produce a higher sensitivity than ^{6}Li with a thermal-neutron cross section of 941 barns, ^{6}Li produces a higher response as demonstrated by the data in Figure 6. (Ruddy, *et al.* 1996) The count rate for $Zr^{10}B_2$ levels off at about 1 μm, while the count rate for ^{6}LiF increases over the entire range of the measurements. The increasing ^{6}LiF sensitivity compared to $Zr^{10}B_2$ is a result of the greater range of the ^{6}Li reaction products (2.73-MeV ^{3}H plus 2.05-MeV ^{4}He) compared to ^{10}B (0.84-MeV ^{7}Li plus 1.47-MeV ^{4}He).

A calculation of the relative neutron sensitivity as a function of ^{6}LiF thickness using the SRIM code (Ziegler & Biersack, 1996) is shown in Figure 7 (Ruddy, *et al.* 1996). The neutron sensitivity levels off at thicknesses greater than 20 μm as a result of the fact that the 2.73 MeV tritons from the ^{6}Li(n,α)^{3}H reaction have a range of 25 μm in LiF. Use of LiF converter layers thicker than 25 μm will not increase the neutron sensitivity and will, in fact, decrease it as a result of thermal neutron absorption by the ^{6}Li in the LiF layer. Thermal neutron attenuation is about 10% at 20 μm and increases rapidly with LiF thickness (Ruddy, *et al.*, 1996).

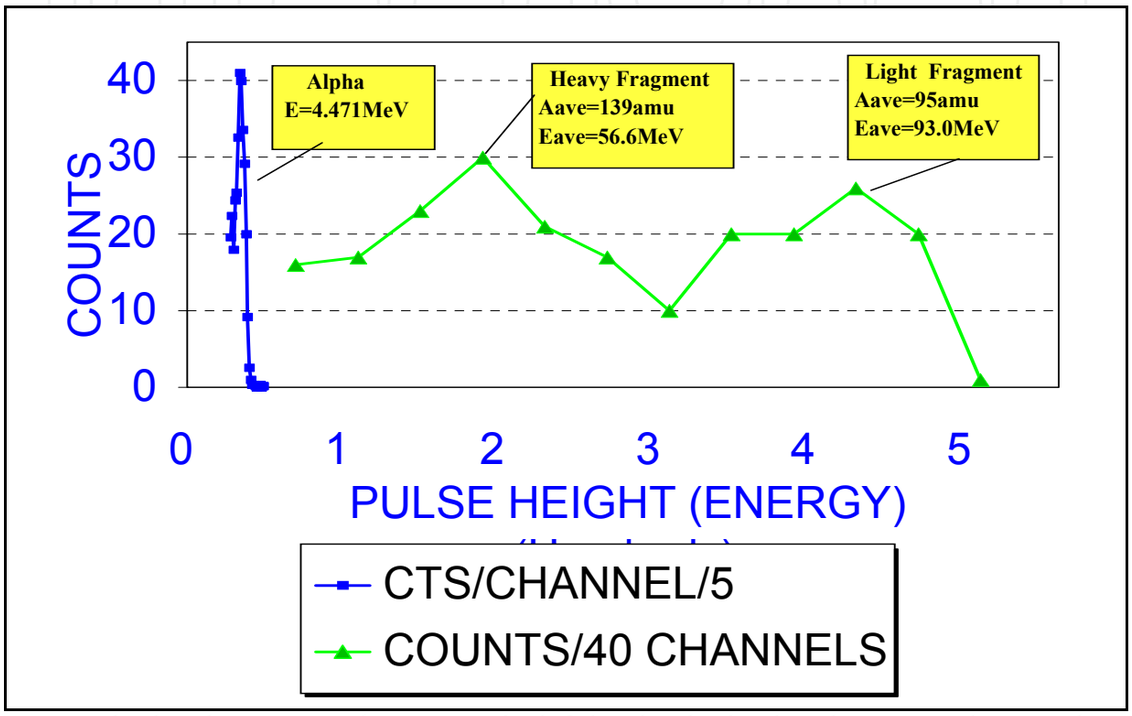

Fig. 5. Pulse height response for a 3-μm thick Schottky diode placed next to a thin ^{235}U layer and exposed to thermal neutrons (data from Ruddy, *et al.*, 1996).

Other materials containing ^{6}Li can provide greater neutron sensitivity than LiF if the range of the neutron-induced tritons in the material is greater than in LiF. A listing of materials with greater triton ranges is contained in Table 1 (Ruddy, *et al.*, 2000). A calculation of neutron sensitivity as a function of layer thickness for each of these materials is shown in Figure 8. The relative sensitivity increases proportionally with the number of tritons escaping the material layer. It can be seen that the relative sensitivity can be increased by factors of two and 4 for LiH and Li, respectively, if used instead of LiF. However, these materials may be less suitable for use in a neutron detector because of their chemical properties. For example, Li is a highly reactive alkali metal and would need to be passivized by encapsulation within a layer of a less reactive metal. LiH is chemically unstable and likely not suitable for use in a neutron detector (Ruddy, *et al.*, 2000).

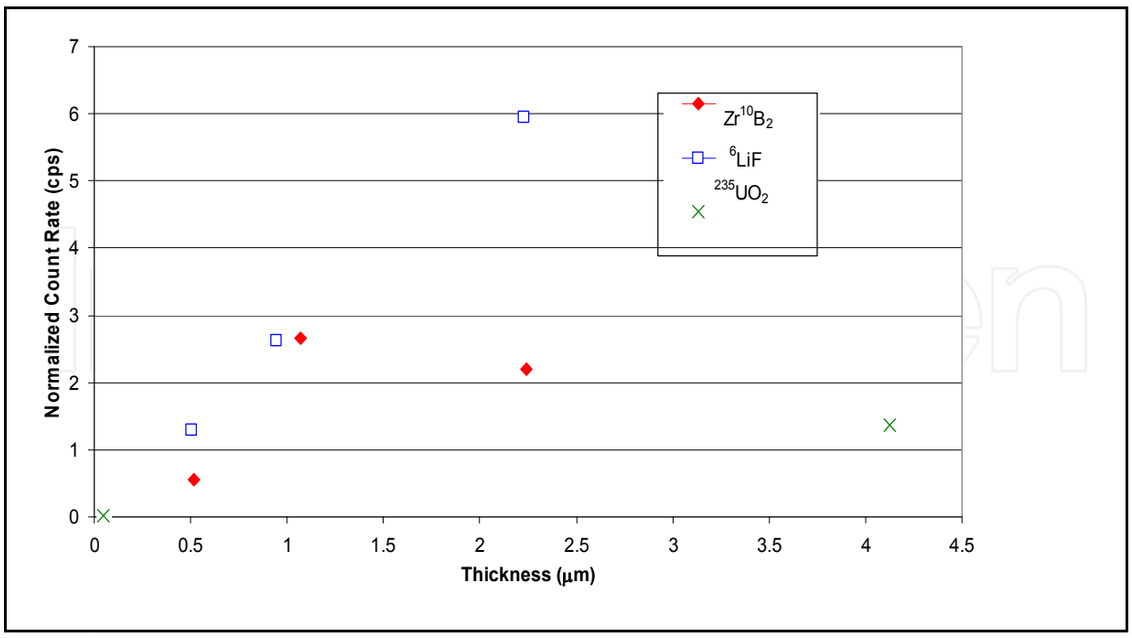

Fig. 6. Count rate as a function of thickness for selected thermal-neutron converter materials (data from Ruddy, *et al.,* 1996).

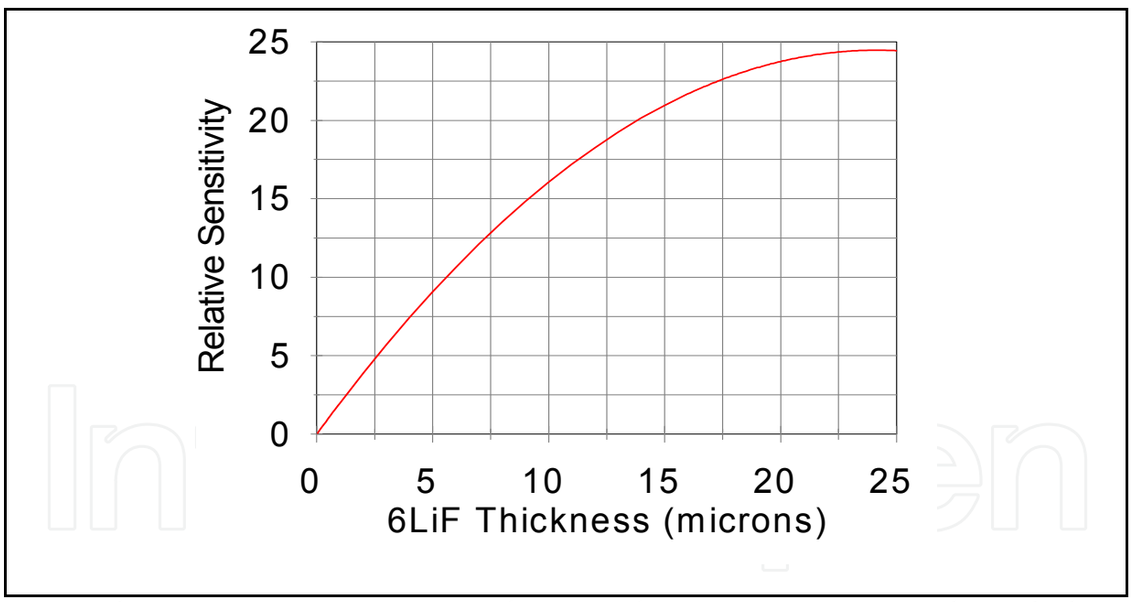

Fig. 7. Relative neutron sensitivity as a function of ^{6}LiF neutron converter layer thickness (data from Ruddy, *et al.,* 1996).

Material	**Range (μm)**
Li	117.88
LiH	60.4
Li_3N	51.95
Li_2C_2	41.58
Li_2O	35.87
LiF	30.77

Table 1. Triton Ranges in Different Materials Containing ^{6}Li (calculations from Ruddy, *et al.*, 2000).

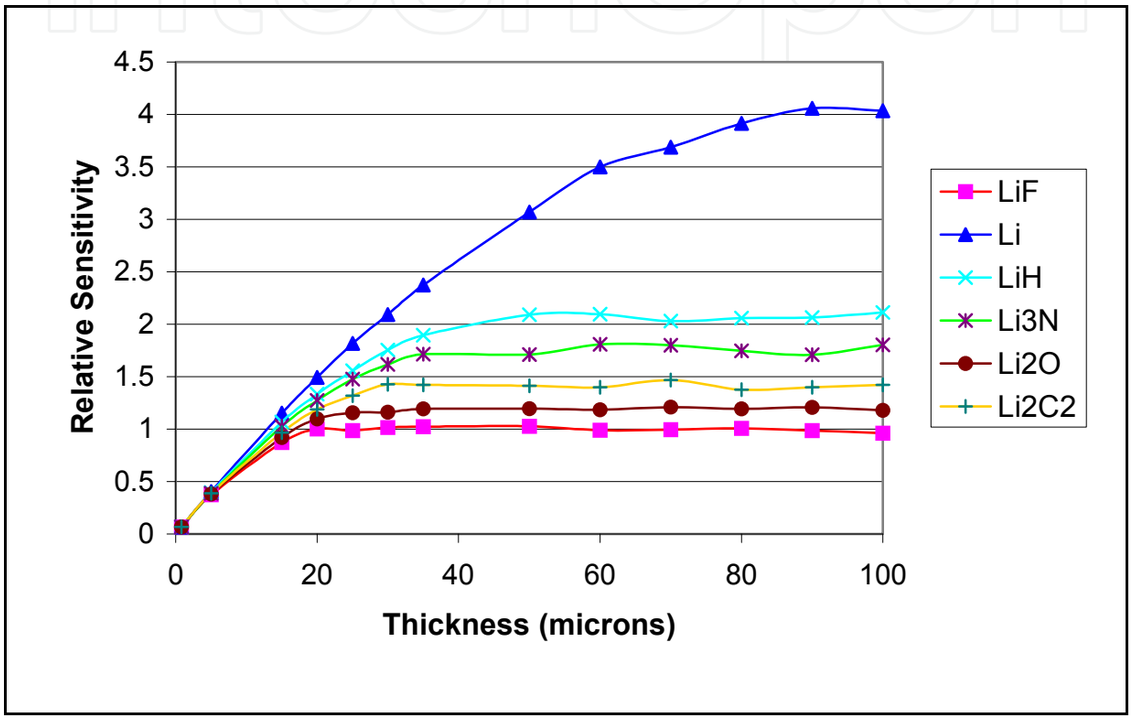

Fig. 8. Relative neutron sensitivity as a function of layer thickness for various materials containing ^{6}Li (calculations from Ruddy, *et al.*, 2000).

3.3 Silicon Carbide Fast Neutron Detectors

At the high energy range pertaining to fast neutrons, several neutron-induced threshold reactions directly with the Si and C atoms of the detector become viable. These reactions lead to the creation of ionizing particles within or close to the detector active volume which carry part of the kinetic information of the incoming neutron thereby enabling neutron detection and, to some extent, neutron spectroscopy. These fast-neutron induced reactions include:

$$^{28}Si + n \rightarrow {}^{28}Si + n'$$
$$^{12}C + n \rightarrow {}^{12}C + n'$$
$$^{28}Si + n \rightarrow {}^{28}Al + p$$
$$^{12}C + n \rightarrow {}^{12}B + p$$
$$^{28}Si + n \rightarrow {}^{25}Mg + {}^{4}He$$
$$^{12}C + n \rightarrow {}^{9}Be + {}^{4}He$$

The list includes only the most prevalent fast-neutron reactions in SiC. Other more complex reactions resulting in the emission of two or more particles will also occur. Also, reactions are listed only for the most abundant Si and C isotopes in the natural elements. Silicon consists of 92.23% ^{28}Si, 4.87% ^{29}Si and 3.10% ^{30}Si. Carbon consists of 98.90% ^{12}C, 1.10% ^{13}C and a negligible amount of ^{14}C. Fast-neutron reactions similar to those listed above can occur with the less abundant isotopes.

The first two reactions listed include elastic and inelastic neutron scattering. In elastic scattering, the neutron interacts with the target nucleus and transfers a variable fraction of its momentum while preserving the overall kinetic energy of the two particles. In inelastic scattering, the neutron elevates the target nucleus to an excited state and transfers momentum without preserving the kinetic energy of the system. The ^{28}Si or ^{12}C recoil atoms are energetic charged particles, which can produce ionization in the active layer of the SiC detector. The secondary neutrons resulting from these reactions however generally escape from the system before inducing any further reactions due to the combined effects of low cross sections and small detector volume. In both elastic and inelastic scattering, the amount of kinetic energy transferred to the ionizing particle is not fixed and a continuum of recoil ion energies will result in the response. While this continuum makes fast-neutron detection still possible, it will not convey an adequate amount of information to infer the energy of the incoming neutron. This is enabled by the other reactions listed above, as discussed in Section 5.

The last four reactions listed result in charged particles, which will all produce ionization in the detector active volume. If the incident fast-neutron energy is monoenergetic, these reactions will produce a fixed response, and a peak will be observed in the pulse-height response spectrum. Such reaction peaks have been observed for SiC and will be discussed in Section 4.2.

The sensitivity for any detector that responds directly to fast neutrons, such as SiC, can be enhanced by juxtaposing a neutron converter layer. Generally, the most effective converter is a layer containing a hydrogenous material, such as polyethylene, because of the high fast –neutron cross section for ^{1}H and the large recoil ranges of the protons produced via the following neutron scattering reaction:

$$^{1}H + n \rightarrow {}^{1}H + n'$$

The recoil protons can produce ionization in the detector active volume and add to the detector response.

SiC fast-neutron response measurements using hydrogen converter layers were carried out by Flammang, *et al.*, 2007.

4. Neutron Response Measurements

4.1 Thermal and Epithermal Neutron Response Measurements

SiC thermal-neutron response measurements have been performed (Dulloo, *et al.*, 1999a; Dulloo, *et al.*, 2003). SiC Schottky diodes with 200μm and 400μm diameters and 3μm thick

active layers were used. Converter layers with 6LiF thicknesses of 8.28 μm and 0.502 μm were used. These measurements demonstrated that when compared to United States National Institute for Standards & Technology (NIST) measurements in NIST standard neutron fields, thirty SiC thermal-neutron responses were linear over neutron fluence-rates ranging from 1.76 x 10^4 cm^{-2} s^{-1} to 3.59 x 10^{10} cm^{-2} s^{-1}. The relative precision of the measurements over this range was ±0.6%. The measurements also demonstrated that pulse-mode operation with discrimination of gamma-ray pulses was possible in a gamma-ray field of approximately 433 Gy Si h^{-1} at a thermal-neutron fluence rate of 3.59 x 10^{10} cm^{-2} s^{-1}. In addition, the thermal-neutron response of a SiC neutron detector previously irradiated with a fast-neutron (E > 1 MeV) fluence of 1.3 x 10^{16} cm^{-2} was indistinguishable from that of an unirradiated SiC detector. The NIST measurements and additional low fluence rate measurements using a ^{252}Cf source are shown in Figure 9. With the ^{252}Cf source results, the linear response spans nine orders of magnitude in fluence rate.

The thermal-neutron response of a prototype SiC ex-core neutron detector was shown to be linear over eight orders of magnitude in neutron fluence rate at the Cornell University Reactor by Ruddy, *et al.*, 2002.

The epithermal response of SiC detectors was measured using cadmium covers by Dulloo, *et al.* 1999b. The epithermal-neutron response was linear as a function of reactor power over the range from 50 watts to 293 watts at the Penn State Brazeale reactor. The relative response of SiC detectors compared to the reactor power instrumentation over the range of the measurements was ±1.7%.

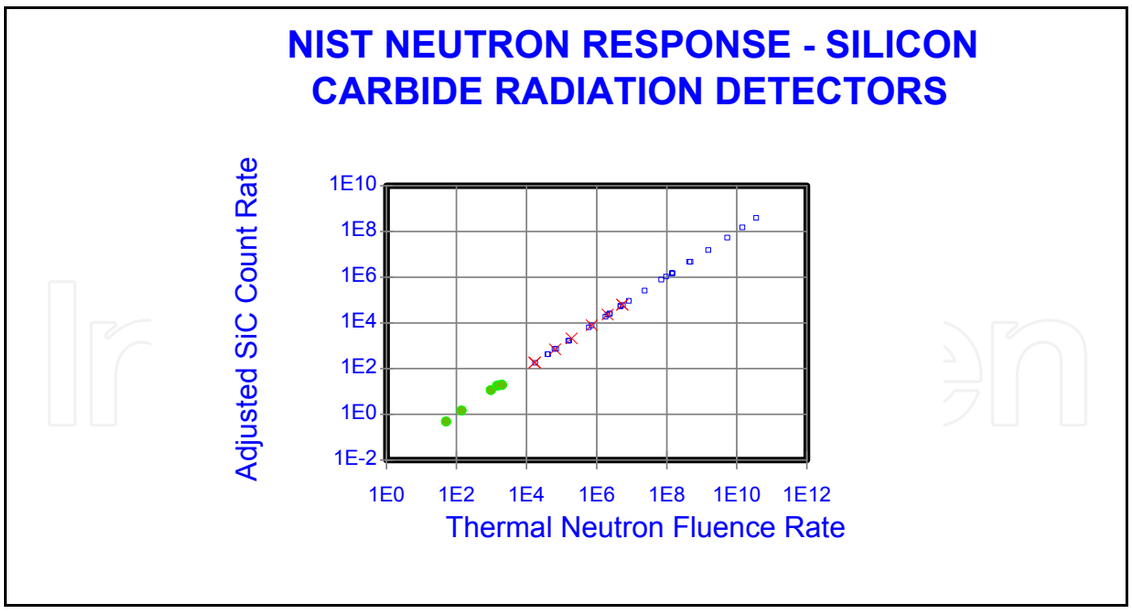

Fig. 9. Silicon Carbide detector response as a function of incident thermal-neutron fluence rate. The NIST response results for an unirradiated SiC detector are shown in blue. The NIST response results for a detector previously irradiated with a fast-neutron (E>1 MeV) fluence of 1.3 x 10^{16} cm^{-2} are shown in red. The response results for thermalized neutrons from a ^{252}Cf source are shown in green.

4.2 Fast-Neutron Response Measurements

Fast-neutron response measurements to ^{252}Cf fission neutrons (E_{AVE} = 2.15 MeV), ^{241}Am-Be (α, n) neutrons (E_{AVE} = 4.5 MeV), 14 MeV neutrons from an electronic deuterium-tritium neutron generator and cosmic-ray induced neutrons were carried out by Ruddy, *et al.*, 2003. A Schottky diode SiC detector with a 28 mm^2 area and a 10 μm active-volume thickness was used without a proton-recoil converter layer. The results are shown in Figure 10.

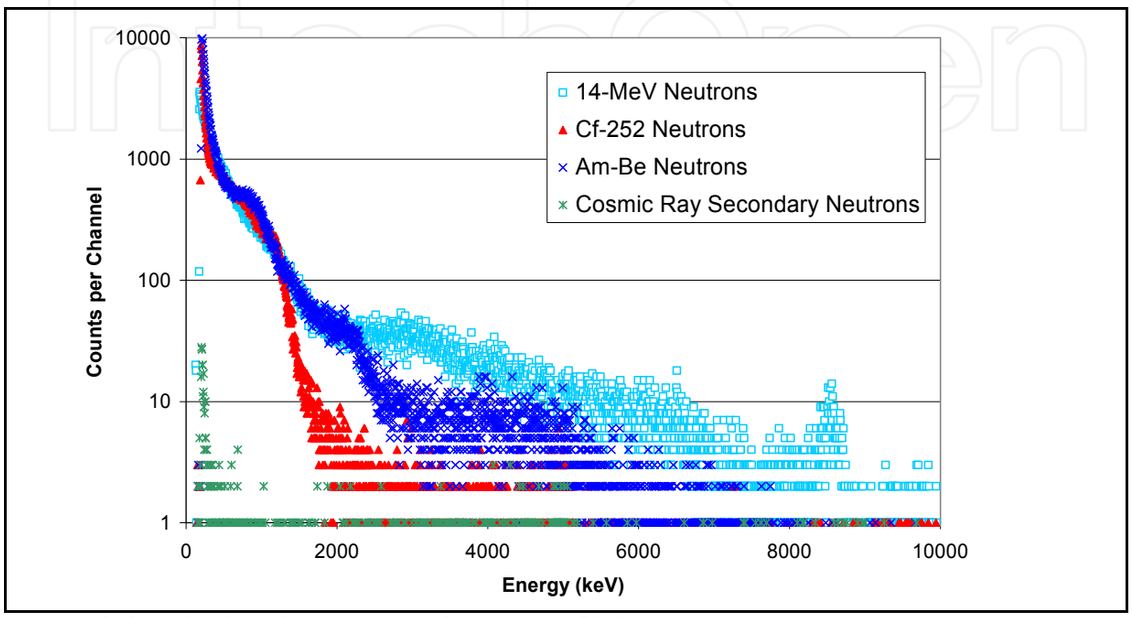

Fig. 10. SiC pulse-height response data for ^{252}Cf fission neutrons, ^{241}Am-Be (α,n) neutrons, 14-MeV neutrons, and cosmic-ray induced background neutrons. (Data reprinted from reference Ruddy, *et al.*, 2003 with permission from the Editorial Department of World Publishing Company Pte. Ltd.)

The pulse-height response spectra clearly shift to higher pulse-heights as a function of incident neutron energy, and structural features corresponding to fast-neutron induced reactions in SiC are visible in the 14-MeV response spectrum. The fast-neutron response measurements were limited by the 10 μm thickness of the SiC detector active volume. Many of the recoil ions that are produced by 14 MeV neutrons have ranges in SiC that are greater than 10 μm and will deposit a variable amount of energy outside of the detector active volume. This lost energy will not contribute to the detector pulse height spectrum and the recovered energy will show in the form of a continuum.

A more detailed examination of the SiC detector response to 14-MeV neutrons is reported in Ruddy *et al.*, 2009a. A 28.3 mm^2 x 100 μm Schottky diode was used without a proton-recoil converter layer. The 100 μm active layer thickness allows much more of the neutron-induced recoil ion energy to be deposited within the active volume of the detector. The resulting 14 MeV pulse-height response data are shown in Figure 11. With the thicker active volume, many more response peaks from fast-neutron reactions become apparent. A listing of the expected nuclear reactions and threshold neutron energies is contained in Table 2.

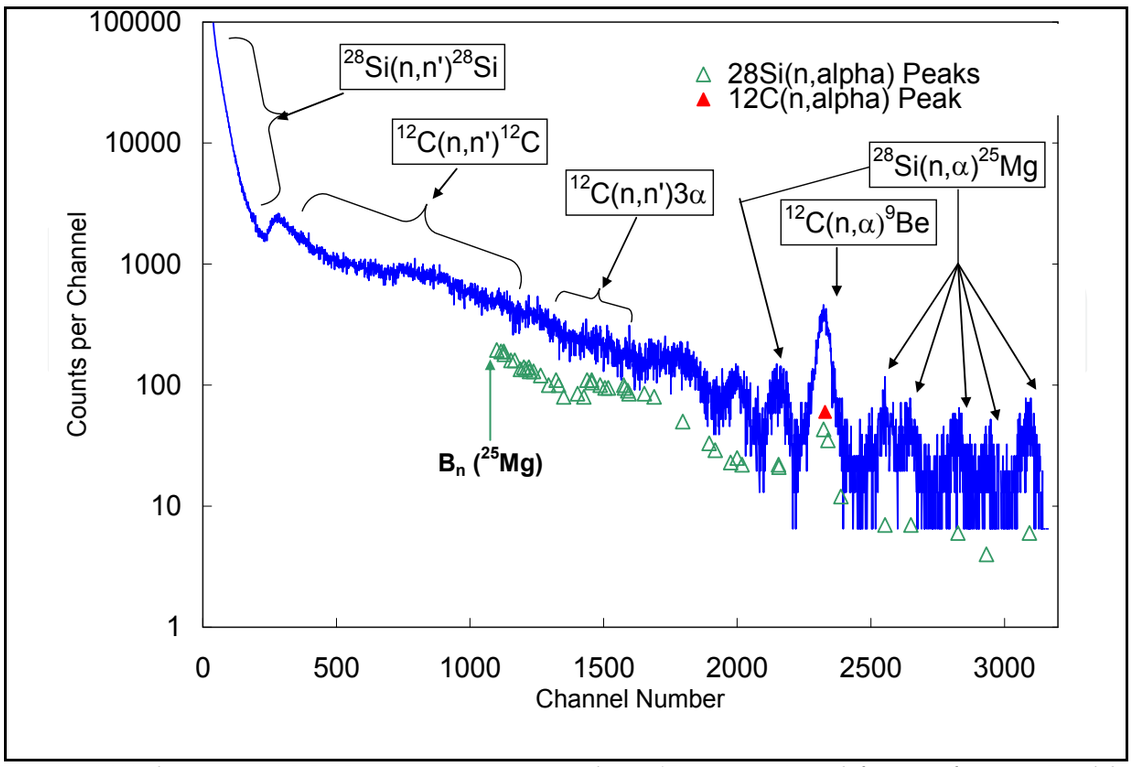

Fig. 11. SiC detector 14 MeV neutron response data. (Data reprinted from reference Ruddy, *et al.,* 2009 with permission from the Editorial Department of World Publishing Company Pte. Ltd.) Channel number is directly proportional to energy deposited in the SiC active volume.

Reaction	Neutron Energy Threshold (MeV)
$^{28}Si(n,n')^{28}Si$	0
$^{28}Si(n,n')^{28*}Si$ (first excited state)	1.843
$^{28}Si(n,\alpha)^{25}Mg$	2.749
$^{28}Si(n,p)^{28}Al$	3.999
$^{12}C(n,n')^{12}C$	0
$^{12}C(n,n')^{12*}C$ (first excited state)	4.809
$^{12}C(n,n')^{12*}C$ (second excited state)	8.292
$^{12}C(n,n')^{12*}C$ (third excited state)	11.158
$^{12}C(n,n')^{12*}C$ (fourth excited state)	13.769
$^{12}C(n,\alpha)^{9}Be$	6.180
$^{12}C(n,n')3\alpha$	7.886
$^{12}C(n,p)^{12}B$	13.643

Table 2. Fast Neutron Reactions in Silicon Carbide.

Only the neutron reactions possible with 14 MeV neutrons are shown in Table 2. Inelastic neutron scattering reactions are shown only for excited states that are bound with respect to particle emission.

At the low-energy portion of the spectrum, the continua for ^{28}Si and ^{12}C elastic and inelastic scattering dominate the detector response shown in Figure 11. At higher energies, specific reaction peaks dominate. The most prominent of these is for the ^{12}C(n,α)^{9}Be reaction, which produces a total of 8.3 MeV in recoil-ion energy.

Several peaks corresponding to the ^{28}Si(n,α)^{25}Mg reaction are observed. The highest-energy (channel number) peak corresponds to the production of ^{25}Mg in its ground state with a total recoil-ion energy of 11.3 MeV. Satellite peaks, corresponding to the production of excited states of ^{25}Mg can be seen at lower energies. The expected positions of these peaks are indicated by green diamonds. Peaks for the first four excited states are clearly visible.

Peaks for the 5th, 6th and 7th excited states are obscured by the ^{12}C(n,α)^{9}Be peak. Evidence for the 8th through 12th excited states is present in the form of unresolved energy peaks. Higher excited states are more closely spaced in energy and blend into a continuum. Eventually, secondary neutron emission becomes possible in ^{25}Mg, which reduces the possibility of observing higher-energy ^{25}Mg excited states.

A comparison of the SiC 14 MeV response with that of a Si passivized ion implanted detector with the same active volume thickness is shown in Figure 12.

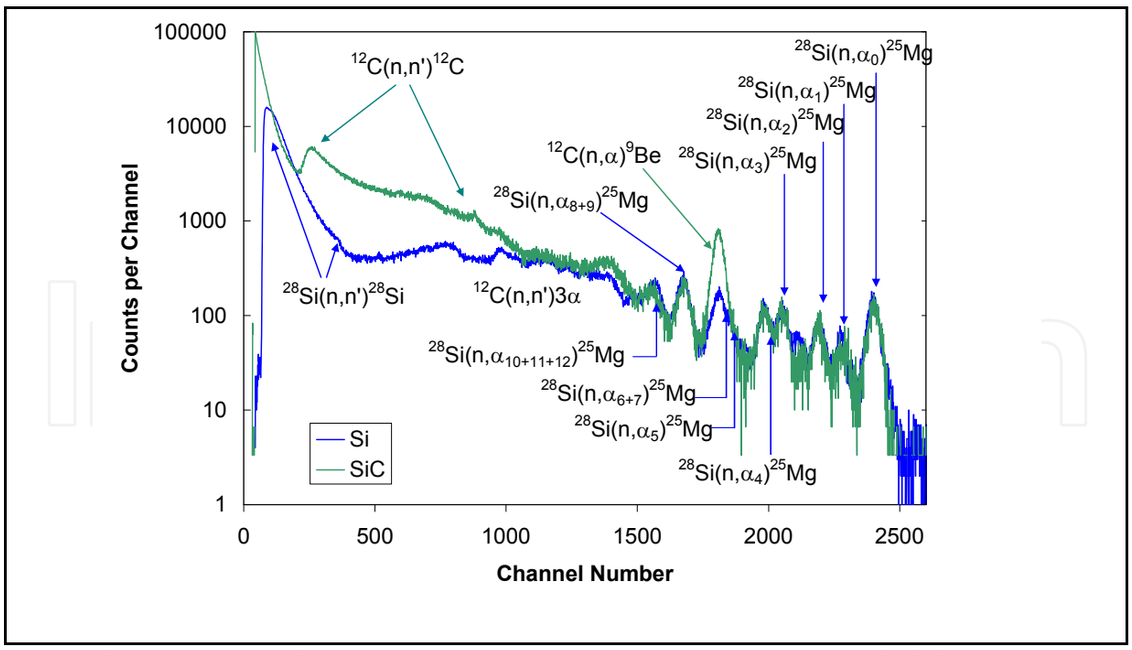

Fig. 12. Comparison of the neutron responses of a 28.3 mm^2 x 100 µm SiC detector and 450 mm^2 x 100 µm Si detector. (Data reprinted from reference Ruddy, *et al.* 2009a with permission from the Editorial Department of World Publishing Company Pte. Ltd.)

The major differences between the two spectra result from the fact that the neutron-induced reactions in carbon are of course absent in the Si detector spectrum. A more detailed comparison of the high-energy peaks is shown in Figure 13. It can be seen that energy positions, peak heights and peak widths are closely matched for the Si and SiC detectors.

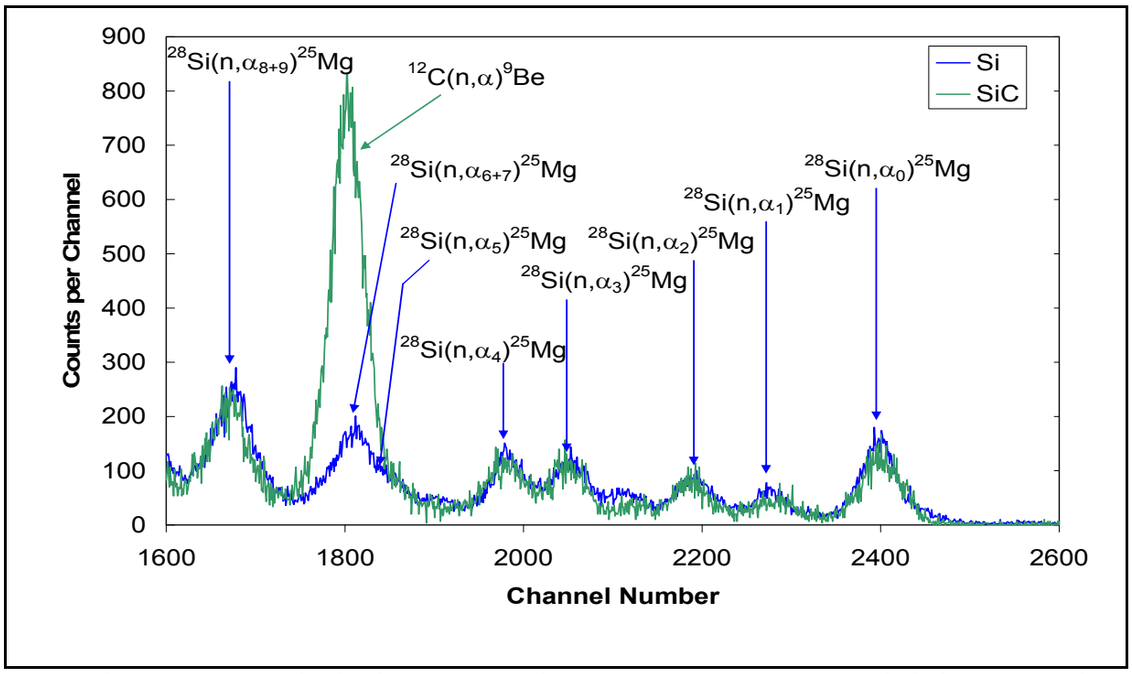

Fig. 13. Comparison of the high-energy peaks in a 28.3 mm² x 100 µm SiC detector and 450 mm² x 100 µm Si detector. (Data reprinted from reference Ruddy, *et al.,* 2009a with permission from the Editorial Department of World Publishing Company Pte. Ltd.)

The response to carbon reactions for the SiC detector can be derived by subtracting the silicon spectrum from the SiC spectrum as shown in Figure 14 (Ruddy, *et al.*, 2009a). The carbon spectrum contains primarily the $^{12}C(n,\alpha)^{9}Be$ peak and continua from neutron elastic and inelastic scattering and multi-particle breakup.

The fast neutron response of SiC detectors to fission neutrons in a reactor was measured by Ruddy, *et al.*, (2006). Three 500 µm diameter x 3 µm SiC Schottky diodes were used to monitor both thermal and fast fission neutron response as a function of reactor power. Two diodes equipped with 24.2 µm and 2.5 µm ^{6}LiF convertor layers were used to monitor thermal neutron response, and the third detector with no convertor layer was used to monitor fast neutrons. The detectors were placed in a beam port at the Ohio State University Research Reactor. Measurements were carried out in the power range from 100 watts to 2000 watts. The SiC fast fission-neutron response compared to the reactor instrumentation was linear over the entire range with a relative standard deviation of $\pm$0.6%.

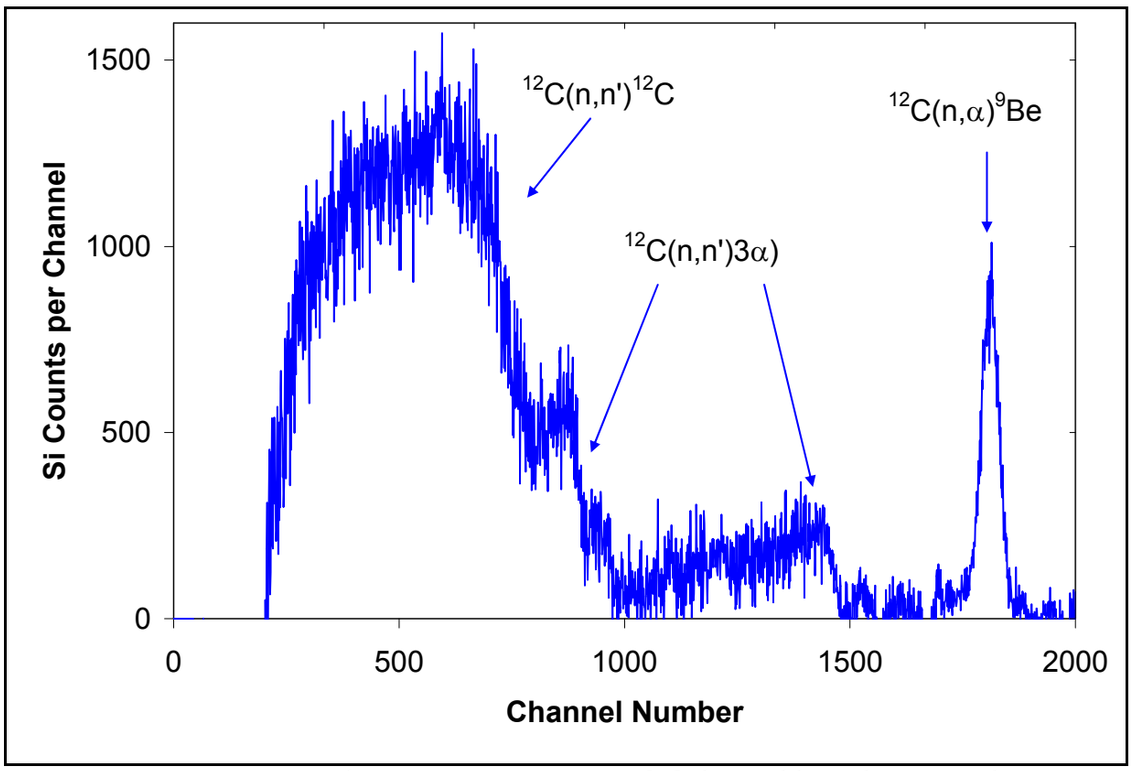

Fig. 14. Response spectrum for 14-MeV reactions in SiC derived by subtracting the response in a Si detector. (Data reprinted from reference Ruddy, *et al.* 2009a with permission from the Editorial Department of World Publishing Company Pte. Ltd.)

The thermal and fast SiC responses were also compared. The relative standard deviation for the measurements at 1000 watts and 2000 watts was $\pm$0.18%.

In a limited set of measurements, SiC detector current was shown to be proportional to reactor power (Ruddy, *et al.*, [2006]).

5. Modeling of the Fast-Neutron Response in Silicon Carbide Neutron Detectors

Modeling of the fast-neutron response of SiC detectors was carried out by Franceschini *et al.*, 2009. A computer code, Particle Generator for SiC (PGSC) was developed to model fast-neutron interactions with SiC and linked to SRIM to streamline the ensuing radiation deposition analysis of the outgoing charged particles. The PGSC code employs a Monte Carlo approach to simulate the particle generation from fast-neutron reactions in the SiC detector active volume, with nuclear cross-section and angular distribution data processed from the ENDF/B-VII.0 data file (ENDF/B-VII.0, 2008). As a result, the collection of possible reactions undergone by source neutrons within SiC is properly sampled and energy, direction and position of the outgoing reaction products can be assigned. The energy deposition of the charged particles is then calculated using the SRIM range-energy code (Ziegler & Biersack, 2006) executed within the PGSC code.

Initial PGSC calculations simulated the response to 14-MeV neutrons for comparison to the measurements by Ruddy, *et al.*, 2009. The (n,p) and (n,α) reactions with C and Si nuclei have been singled out in the prediction by the PGSC code and fitted with Gaussian curves, as shown in Figure 15. Peaks from the (n,α) reactions account for the bulk of the response with the $^{12}C(n,\alpha)^{9}Be$ ground-state reaction peak most prominent. The $^{28}Si(n,\alpha)^{25}Mg$ ground state peak and fifteen ^{25}Mg excited states peaks are also visible. Peaks from the ground state and thirteen ^{28}Al excited states for the $^{28}Si(n,p)^{28}Al$ reaction are also apparent. The (n,p) peaks are limited by the fact that much of the proton energy is deposited outside of the detector active volume.

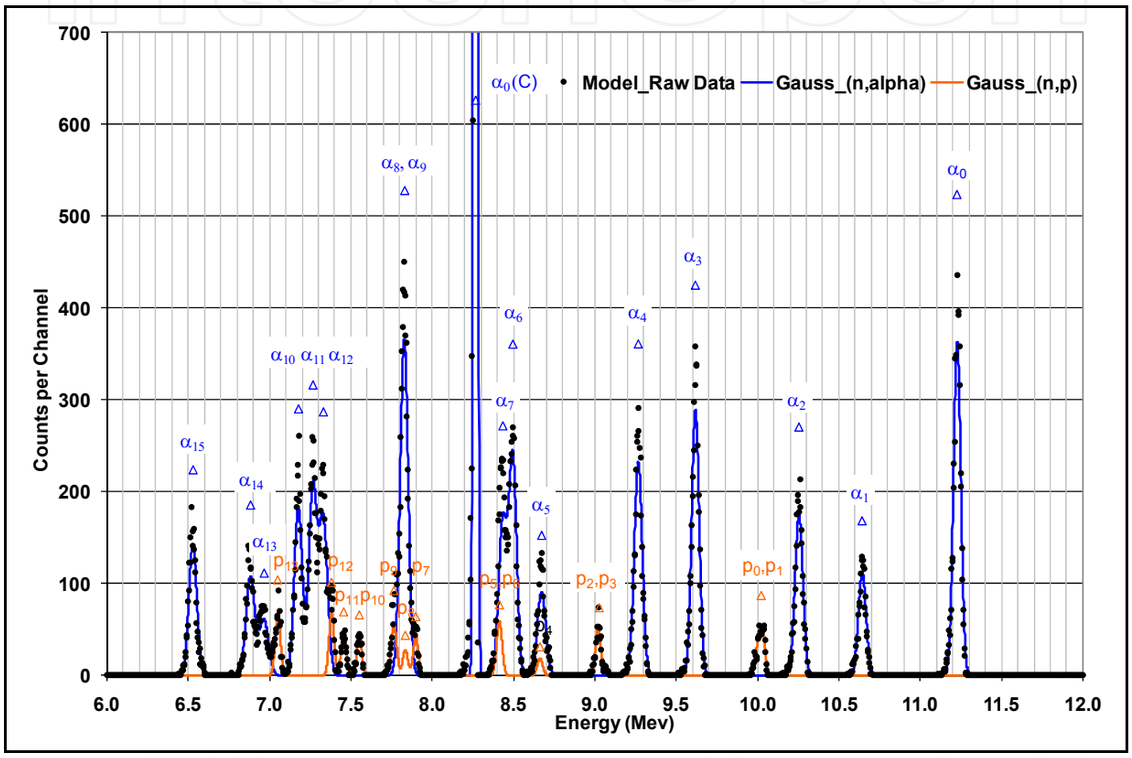

Fig. 15. Predicted SiC Detector Response. Raw Data and Gaussian Interpolations for (n,p) and (n,α) reactions. (Data reprinted from Franceschini *et al.*, 2009 with permission from the Editorial Department of World Publishing Company Pte. Ltd.)

A comparison of the predicted and measured (Ruddy, *et al.*, 2009a) detector responses is shown in Figure 16. A Gaussian representation of the calculated response is compared to the measured data points. The peak positions and intensities match well. The peak widths are narrower for the predicted response than for the measured response. This is likely a result of limitations in the SRIM code.

The eventual goal for the PGSC code is to develop a neutron response spectrum de-convolution methodology, which will allow neutron energy spectra determination for downscattered fission neutrons in complex nuclear reactor environments.

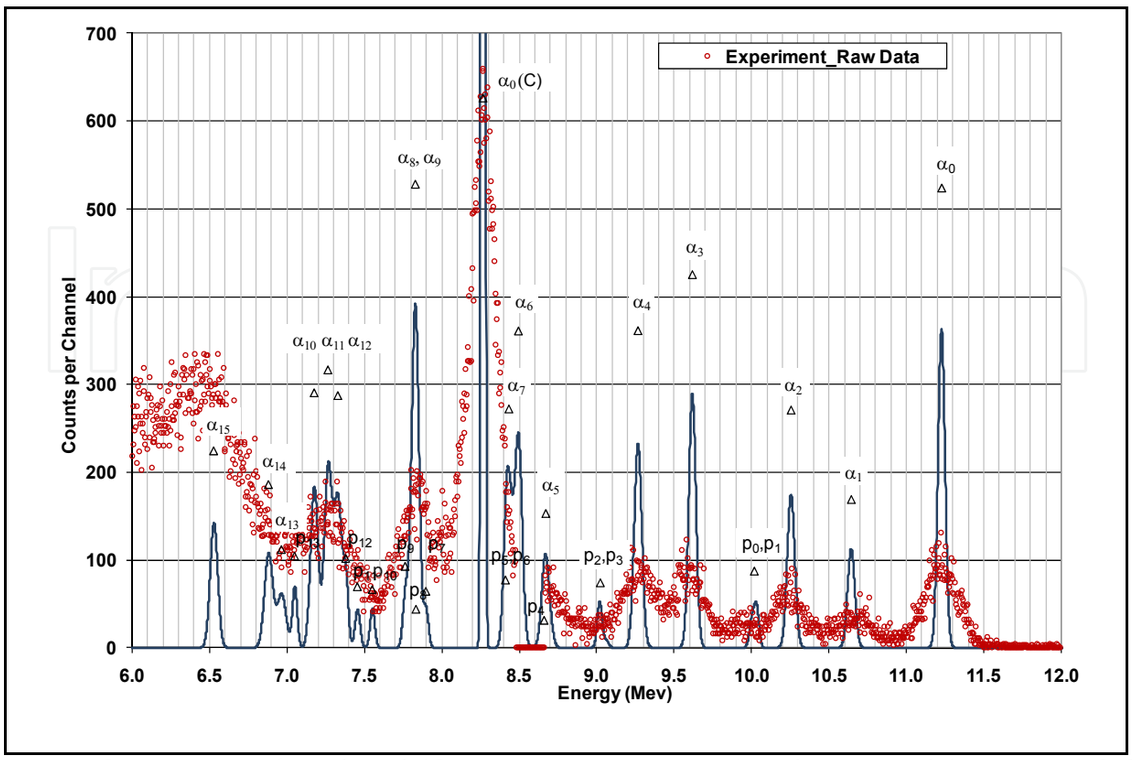

Fig. 16. Comparison of predicted (Gaussian Representation) and Measured (Raw Data) SiC detector responses. (Data reprinted from Franceschini *et al.*, 2009 with permission from the Editorial Department of World Publishing Company Pte. Ltd.)

6. Discussion and Conclusions

Silicon carbide neutron detectors are ideally suited for nuclear reactor applications where high-temperature, high-radiation environments are typically encountered. Among these applications are reactor power-range monitoring (Ruddy, *et al., 2002)*. Fast-neutron fluences at ex-core reactor power-range monitor locations are approximately 10^{17} n cm^{-2}. Semiconductor detectors such as those based on Si or Ge cannot withstand such high fast-neutron fluences and would be unsuitable for this application.

Epitaxial SiC detectors have been shown to operate at temperatures up to 375 ^{o}C (Ivanov, *et al.*, 2009). Temperatures do not exceed 350 ^{o}C in conventional and advanced pressurized water reactor designs. Therefore, SiC neutron detectors should prove useful for applications in these environments. SiC neutron detectors can potentially be used in reactor monitoring locations with temperatures up to 700 ^{o}C (Babcock, *et al.*, 1957; Babcock & Chang, 1963). Such temperatures can be encountered in advanced gas-cooled or liquid-metal cooled reactors. At such temperatures, the long-term integrity of the detector contacts is the key issue rather than the performance of the SiC semiconductor.

Other potential reactor monitoring applications are in-vessel neutron detectors (Ruddy, *et al.*, 2002), monitoring in proposed advanced power reactors (Petrović, *et al.*, 2003) and monitoring of reactors aboard outer space vehicles (Ruddy, *et al.*, 2005).

SiC detectors have also been used to monitor neutron exposures in Boron-Capture Neutron Therapy (Manfreddoti, *et al.*, 2005) as well as the thermal-neutron fluence rates in prompt-gamma neutron activation of waste drums (Dulloo, *et al.*, 2004).

SiC detectors have proven useful for neutron interrogation applications to detect concealed nuclear materials for Homeland Security applications (Ruddy, *et al.*, 2007; Blackburn, *et al.*, 2007; Ruddy, *et al.*, 2009c).

An application that is particularly well suited for SiC detectors is monitoring of spent nuclear fuel. Spent-fuel environments are characterized by very high gamma-ray intensities of the order of 1,000 Gy/hr and very low neutron fluence rates of the order of hundreds per cm^2 per second. Measurements were carried out in simulated spent fuel environments (Dulloo, *et al.*, 2001), which demonstrated the excellent neutron/gamma discrimination capability of SiC detectors. Long-term monitoring measurements were carried out on spent-fuel assemblies over a 2050 hour period, and regardless of the total gamma-ray dose to the detector of over 6000 Gy, the detector successfully monitored both gamma-rays and neutrons with no drift or changes in sensitivity over the entire monitoring period (Natsume, *et al.*, 2006).

SiC detectors have been shown to operate well after a cumulative ^{137}Cs gamma-ray dose of 22.7 MGy (Ruddy & Seidel, 2006; Ruddy & Seidel, 2007). This gamma-ray dose exceeds the total dose that a spent fuel assembly can deliver after discharge from the reactor indicating that cumulative gamma-ray dose to a SiC detector will never be a factor for spent-fuel monitoring applications.

The rapid pace of SiC detector development and the large number of research groups involved worldwide bode well for the future of SiC detector applications.

7. References

Babcock, R. ; Ruby, S. ; Schupp, F. & Sun, K (1957) Miniature Neutron Detectors, Westinghouse Electric Corporation Materials Engineering Report No. 5711-6600-A (November, 1957)

Babcock, R. & Chang, H. (1963) Silicon Carbide Neutron Detectors for High-Temperature Operation, In : *Reactor Dosimetry*, Vol. 1 , p 613 International Atomic Energy Agency, Vienna, Austria.

Bertuccio, G.; Casiraghi, R & Nava, F. (2001) Epitaxial Silicon Carbide for X-Ray Detection, *IEEE Transactions on Nuclear Science*, Vol. 48, pp 232-233.

Bertuccio, G. & Casiraghi, R. (2003) Study of Silicon Carbide for X-Ray Detection and Spectroscopy, *IEEE Transactions on Nuclear Science*, Vol. 50, pp 177-185.

Bertuccio, G.; Casiraghi, R.; Cetronio, A.; Lanzieri, C. & Nava, F. (2004a) A New Generation of X-Ray Detectors Based on Silicon Carbide, *Nuclear Instruments & Methods in Physics Research A*, Vol. 518, pp 433-435.

Bertuccio, G.; Casiraghi, R.; Centronio, A,; Lanzieri, C. & Nava, F. (2004b) Silicon Carbide for High-Resolution X-Ray Detectors Operating Up to 100 ^{o}C, *Nuclear Instruments & Methods in Physics Research A*, Vol. 522, pp 413-419.

Bertuccio, G.; Binetti, S.; Caccia, S.; Casiraghi, R.; Castaldini, A.; Cavallini, A.; Lanzieri, C.; Le Donne, A.; Nava, F.; Pizzini, S.; Riquutti, L & Verzellesi, G. (2005) Silicon Carbide for Alpha, Beta, Ion and Soft X-Ray High Performance Detectors. *Silicon Carbide and Related Materials 2004. Materials Science Forum* Vols. 483-485, pp 1015-1020.

Bertuccio, G.; Caccia, S.; Puglisi, D. & Macera, M (2010 Advances in Silicon Carbide X-Ray Detectors, *Nuclear Instruments & Methods in Physics Research A*, In press (available on-line).

Blackburn, B.; Johnson, J..; Watson, S.; Chichester, D.; Jones, J.; Ruddy, F.; Seidel, J. & Flammang, R. (2007) Fast Digitization and Discrimination of Prompt Neutron and Photon Signals Using a Novel Silicon Carbide Detector, *Optics and Photonics in Global Homeland Security* (Saito, T. *et al.* Eds.) *Proceedings of SPIE – The International Society for Optical Engineering*, Vol. 6540, Paper 65401J.

Bruzzi, M.; Lagomarsino, S.; Nava, F. & Sciortino, S. (2003) Characteristics of Epitaxial SiC Schottky Barriers as Particle Detectors, *Diamond and Related Materials*, Vol. 12, pp 1205-1208.

Dulloo, A.; Ruddy, F.; Seidel, J.; Adams, J.; Nico, J. & Gilliam, D (1999a) The Neutron Response of Miniature Silicon Carbide Semiconductor Detectors, *Nuclear Instruments & Methods in Physics Research A*, Vol. 422, pp 47-48.

Dulloo, A.; Ruddy, F.; Seidel, J.; Davison, C.; Flinchbaugh, T. & Daubenspeck, T. (1999b) Simultaneous Measurement of Neutron and Gamma-Ray Radiation Levels from a TRIGA Reactor Core Using Silicon Carbide Semiconductor Detectors, *IEEE Transactions on Nuclear Science,* Vol. 46, pp 275-279.

Dulloo, A.; Ruddy, F.; Seidel, J.; Flinchbaugh, T.; Davison, C. & Daubenspeck, T. (2001) Neutron and Gamma Ray Dosimetry in Spent-Fuel Radiation Environments Using Silicon Carbide Semiconductor Radiation Detectors, In: *Reactor Dosimetry: Radiation Metrology and Assessment* (J. Williams, *et al.*, (Eds.), ASTM STP 1398, American Society for Testing and Materials, West Conshohoken, Pennsylvania, pp 683-690.

Dulloo, A.; Ruddy, F.; Seidel, J.; Adams, J.; Nico, J. & Gilliam, D (2003) The Thermal Neutron Response of Miniature Silicon Carbide Semiconductor Detectors, *Nuclear Instruments & Methods in Physics Research A*, Vol. 498, pp 415-423.

Dulloo, A.; Ruddy, F.; Seidel, J.; Lee, S.; Petrović, B. & McIlwain, M. (2004) Neutron Fluence-Rate Measurements in a PGNAA 208-Liter Drum Assay System Using Silicon Carbide Detectors, *Nuclear Instruments & Methods B*, Vol. 213, pp 400-405.

ENDF/B-VII.0 Nuclear Data File, National Nuclear Data Center, Brookhaven National Laboratory, Upton, NY (on the internet at http://www.nndc.bnl.gov/exfor7/endf00.htm.

Evstropov, V.; Strel'chuk, A.; Syrkin, A. & Chelnokov, V. (1993) The Effect of Neutron Irradiation on Current in SiC pn Structures, *Inst. Physics Conf. Ser.* No.137, Chapter 6, (1993)

Ferber, R. & Hamilton, G. (1965) Silicon Carbide High Temperature Neutron Detectors for Reactor Instrumentation, Westinghouse Research & Development Center Report No. 65-1C2-RDFCT-P3 (June, 1965).

Flammang, R.; Ruddy, F. & Seidel, J. (2007) Fast Neutron Detection With Silicon Carbide Semiconductor Radiation Detectors, *Nuclear Instruments & Methods in Physics Research A,* Vol. 579, pp 177-179.

Franceschini, F.; Ruddy, F. & Petrović, B. (2009) Simulation of the Response of Silicon Carbide Fast Neutron Detectors, In: *Reactor Dosimetry State of the Art 2008,* Voorbraak, W. e*t al.* Eds., World Scientific, London, pp 128-135.

Ivanov, A.; Kalinina, E.; Kholuyanov, G.; Strokan, N.; Onushkin, G.; Konstantinov, A.; Hallen, A. & Kuznetsov, A. (2004) High Energy Resolution Detectors Based on 4H-SiC, In: *Silicon Carbide and Related Materials 2004,* R. Nipoti, *et al.* (Eds.), Materials Science Forum Vols. 483-484, pp 1029-1032.

Ivanov, A.; Kalinina, E.; Strokan, N. & Lebedev, A. (2009) 4H-SiC Nuclear Radiation p-n Detectors for Operation Up to Temperature 375 ºC, *Materials Science Forum*, Vols. 615-617, pp 849-852.

Lees, J.; Bassford, D.; Fraser, G.; Horsfall, A.; Vassilevski, K.; Wright, N. & Owens, A. (2007) Semi-Transparent SiC Schottky Diodes for X-Ray Spectroscopy, *Nuclear Instruments & Methods in Physics Research A*, Vol. 578, pp 226-234.

Lo Giudice, A.; Fasolo, F.; Durisi, E.; Manfredotti, C.; Vittone, E.; Fizzotti, F.; Zanini, A. & Rosi, G. (2007) Performance of 4H-SiC Schottky Diodes as Neutron Detectors, *Nuclear Instruments & Methods in Physics Research A*, Vol. 583, pp 177-180.

Manfredotti, C.; Lo Giudice, A.; Fasolo, F.; Vittone, E.; Paolini, F.; Fizzotti, F.; Zanini, A.; Wagner, G. & Lanzieri, C. (2005) SiC Detectors for Neutron Monitoring, *Nuclear Instruments & Methods in Physics Research A*, Vol. 552, pp 131-137.

Natsume, T.; Doi, H.; Ruddy, F.; Seidel, J. & Dulloo, A. (2006) Spent Fuel Monitoring with Silicon Carbide Semiconductor Neutron/Gamma Detectors, *Journal of ASTM International*, Online Issue 3, March 2006.

Nava, F.; Bertuccio, G.; Cavallini, A. & Vittone, E. (2008) Silicon Carbide and Its Use as a Radiation Detector Material, *Materials Science Technology*, Vol. 19, pp 1-25.

Nava, F.; Vanni, P.; Lanzieri, C. & Canali, C. (1999) Epitaxial Silicon Carbide Charge Particle Detectors, *Nuclear Instruments and Methods in Physics Research A,* Vol. 437, pp 354-358.

Petrović, B.; Ruddy, F. & Lombardi, C. (2003) Optimum Strategy For Ex-Core Dosimeters/Monitors in the IRIS Reactor, In: *Reactor Deosimetry in the 21st Century*, J. Wagemans, *et al.* (Eds.), World Scientific, London, pp 43-50.

Phlips, B.; Hobart, K.; Kub, F.; Stahlbush, R.; Das, M.; De Geronimo, G. & O'Connor, P. (2006) Silicon Carbide Power Diodes as Radiation Detectors, *Materials Science Forum*, Vols. 527-529, pp 1465-1468.

Ruddy, F.; Dulloo, A.; Seshadri, S.; Brandt, C & Seidel, J. (1997) Development of a Silicon Carbide Semiconductor Neutron Detector for Monitoring Thermal Neutron Fluxes, Westinghouse Science & Technology Center Report No. 96-9TK1-NUSIC-R1, July 24, 1996.

Ruddy, F.; Dulloo, A.; Seidel, J.; Seshadri, S. & Rowland, B. (1999) Development of a Silicon Carbide Radiation Detector, *IEEE Transactions on Nuclear Science*, Vol. 45, p 536-541.

Ruddy, F.; Dulloo, A.; Seidel, J.; Edwards, K.; Hantz, F. & Grobmyer, L. (2000) Reactor Ex-Core Power Monitoring with Silicon Carbide Semiconductor Neutron Detectors, Westinghouse Electric Co. Report WCAP-15662, December 20, 2000, reclassified in October 2010.

Ruddy, F.; Dulloo, A.; Seidel, J.; Hantz, F. & Grobmyer, L. (2002) Nuclear Reactor Power Monitoring Using Silicon Carbide Semiconductor Radiation Detectors, *Nuclear Technology* Vol.140, p 198.

Ruddy, F.; Dulloo, A. & Petrović, B. (2003) Fast Neutron Spectrometry Using Silicon Carbide Detectors, In: *Reactor Dosimetry in the 21st Century*, Wagemans, J., *et al.*, Editors, World Scientific, London, pp 347-355.

Ruddy, F.; Patel, J. & Williams, J. (2005) Power Monitoring in Space Nuclear Reactors Using Silicon Carbide, *Proceedings of the Space Nuclear Conference*, CD ISBN 0-89448-696-9 American Nuclear Society, LaGrange, Illinois, pp 468-475.

Ruddy, F. & Seidel, J. (2006) Effects of Gamma Irradiation on Silicon Carbide Semiconductor Radiation Detectors, *2006 IEEE Nuclear Sciences Symposium*, San Diego, California, Paper N14-221.

Ruddy, F.; Dulloo, A.; Seidel, J.; Blue, T. & Miller, D. (2006) Reactor Power Monitoring Using Silicon Carbide Fast Neutron Detectors, *PHYSOR 2006: Advances in Nuclear Analysis and Simulation*, Vancouver, British Columbia, Canada, 10-14 September 2006, American Nuclear Society, Proceedings available on CD-ROM ISBN: 0-89448-697-7.

Ruddy, F.; Seidel, J. & Flammang, R. (2007) Special Nuclear Material Detection Using Pulsed Neutron Interrogation, *Optics and Photonics in Global Homeland Security* (Saito, T. *et al.* Eds.) *Proceedings of SPIE – The International Society for Optical Engineering*, Vol. 6540, Paper 65401I.

Ruddy, F. & Seidel, J. (2007) The Effects of Intense Gamma Irradiation on the Alpha-Particle Respone of Silicon Carbide Semiconductor Radiation Detectors, *Nuclear Instruments & Methods in Physics Research B*, Vol. 263, pp 163-168.

Ruddy, F.; Seidel, J. & Franceschini, F. (2009a) Measurements of the Recoil-Ion Response of Silicon Carbide Detectors to Fast Neutrons, In: *Reactor Dosimetry State of the Art 2008,* Voorbraak, W. e*t al.* Eds., World Scientific, London, pp 77-84.

Ruddy, F.; Seidel, J. & Sellin, P. (2009b) High-Resolution Alpha Spectrometry with a Thin-Window Silicon Carbide Semiconductor Detector, *2009 IEEE Nuclear Science Symposium Conference Record*, Paper N41-1, pp 2201-2206.

Ruddy, F.; Flammang, R. & Seidel, J. (2009c) Low-Background Detection of Fission Neutrons Produced by Pulsed Neutron Interrogation, *Nuclear Instruments & Methods in Physics Research A*, Vol. 598, pp 518-525.

Strokan, N.; Ivanov, A. & Lebedev, A. (2009) Silicon Carbide Nuclear-Radiation Detectors, *SiC Power Materials: Devices and Applications*, (Feng, Z. Ed.) Chapter 11, Springer-Verlag, New York, pp 411-442.

Tikhomirova, V.; Fedoseeva, O. & Kholuyanov, G. (1972) Properties of Ionizing-Radiation Counters Made of Silicon Carbide Doped by Diffusion of Beryllium, *Soviet Physics – Semiconductors* Vol.6, No. 5 (November, 1972)

Tikhomirova, V.; Fedoseeva, O. & Kholuyanov, G. (1973a) Detector Characteristics of a Silicon Carbide Detector Prepared by Diffusion of Beryllium, *Atomnaya Energiya* Vol. 34, No. 2, (February, 1973) pp 122-124.

Tikhomirova, V.; Fedoseeva, O. & Bol'shakov, V. (1973b) Silicon Carbide Detectors as Fission-Fragment Counters in Reactors, *Izmeritel'naya Tekhnika* Vol. 6 (June, 1973) pp 67-68.

Ziegler, J & Biersack, J (1996) SRIM-96: The Stopping and Range of Ions in Matter, IBM Research, Yorktown, New York.

Ziegler, J & Biersack, J (2006) The Stopping and Range of Ions in Solids, 2006 edition, Yorktown, New York (on the Internet at http://www.srim.org)

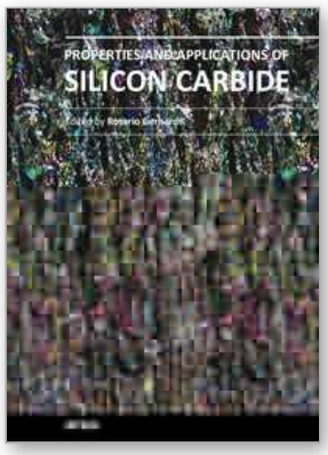

Properties and Applications of Silicon Carbide
Edited by Prof. Rosario Gerhardt

ISBN 978-953-307-201-2
Hard cover, 536 pages
Publisher InTech
Published online 04, April, 2011
Published in print edition April, 2011

In this book, we explore an eclectic mix of articles that highlight some new potential applications of SiC and different ways to achieve specific properties. Some articles describe well-established processing methods, while others highlight phase equilibria or machining methods. A resurgence of interest in the structural arena is evident, while new ways to utilize the interesting electromagnetic properties of SiC continue to increase.

How to reference
In order to correctly reference this scholarly work, feel free to copy and paste the following:

Fausto Franceschini and Frank H. Ruddy (2011). Silicon Carbide Neutron Detectors, Properties and Applications of Silicon Carbide, Prof. Rosario Gerhardt (Ed.), ISBN: 978-953-307-201-2, InTech, Available from: http://www.intechopen.com/books/properties-and-applications-of-silicon-carbide/silicon-carbide-neutron-detectors

INTECH
open science | open minds

InTech Europe
University Campus STeP Ri
Slavka Krautzeka 83/A
51000 Rijeka, Croatia
Phone: +385 (51) 770 447
Fax: +385 (51) 686 166
www.intechopen.com

InTech China
Unit 405, Office Block, Hotel Equatorial Shanghai
No.65, Yan An Road (West), Shanghai, 200040, China
中国上海市延安西路65号上海国际贵都大饭店办公楼405单元
Phone: +86-21-62489820
Fax: +86-21-62489821

© 2011 The Author(s). Licensee IntechOpen. This chapter is distributed under the terms of the Creative Commons Attribution-NonCommercial-ShareAlike-3.0 License, which permits use, distribution and reproduction for non-commercial purposes, provided the original is properly cited and derivative works building on this content are distributed under the same license.

IntechOpen

IntechOpen